Available online at www.sciencedirect.com

ScienceDirect

Procedia Computer Science 89 (2016) 575 – 586

Procedia Computer Science

Twelfth International Multi-Conference on Information Processing-2016 (IMCIP-2016)

Flood Assessment using Multi-Temporal Modis Satellite Images

C. S. Arvind[a,*], Ashoka Vanjare[b], S. N. Omkar[b,*], J. Senthilnath[b], V. Mani[b] and P. G. Diwakar[c]

[a] *Robert Bosch Engineering and Business Solution Private Limited, Bangalore*
[b] *Indian Institute of Science, Bangalore*
[c] *Indian Space Research Organisation, Bangalore*

Abstract

Flood assessment using unsupervised techniques for multi-temporal MODIS satellite images is presented. Classical methods like mean shift algorithm is compared with artificial neural network method like self organizing maps for automatic water pixel identification and extraction. The extracted results help in identification of flooded and non-flooded places. Different methods are applied and comparative study of unsupervised methods involving mean shift and self organizing maps are carried-out. In order to evaluate the algorithmic performance, root mean square error and receiver operating characteristics is used as performance evaluation indices. The results reported will provide useful information for multi-temporal time series satellite image analysis which can be used for current and future research in disasters management.

Peer-review under responsibility of organizing committee of the Organizing Committee of IMCIP-2016

Keywords: Image Segmentation; Mean Shift; MODIS Satellite Images; Receiver of Characteristics; Root Means Square; Self-Organizing Maps; Unsupervised Techniques.

1. Introduction

Multi-temporal time series analyses of satellite images play a vital role in differentiating or discriminating the changes in the areas of land cover between dates of imaging. Researchers continue to develop different tools which can assist in time series analysis for the changes for the same region. Representing a tool[1] is a technique that consists of a set of iterative and interactive steps that aid an analyst in delineating true land cover changes from incidental scene to scene changes. Some of the multi-temporal analysis applications are flood assessment[2], agriculture[3], fuel type assessment[4], and spatial soil moisture mapping[5]. This paper investigates multi-temporal time series analysis of the flood prone area using MODIS satellite images.

In the present study, Multi-temporal images of the flooded scene were used for mapping flooded places and data analysis. Analysis of image segmentation methods yield detailed map of flooded places differentiating from non-flooded places. We have integrated spectral, spatial and contextual information for extraction of flood-prone regions. we have made use of MODIS band 2 satellite image because it clearly discriminates between vegetation

*Corresponding author. Tel.: +91 -9741233008.
E-mail address: csarvind2000@gmail.com

Peer-review under responsibility of organizing committee of the Organizing Committee of IMCIP-2016
doi:10.1016/j.procs.2016.06.017

and water image pixels; the sensor design team recommends MODIS band 2[6] for studying change detection in topography, like flood assessment[6–9] and vegetation. The basic idea of using remote sensing data in studying change detection[10] lies in the fact that the surface reflectance change captured helps to discriminate water image pixels from others in the satellite image which in turn helps in image interpretation. The study of image interpretation helps to distinguish flooded and non-flooded regions[11] from the satellite images. Further for better image interpretation, we have made used pre and post satellite images of the same region. The MODIS data is highly suitable for flood assessment because it is real-time (or nearly real-time) disseminated and inexpensive, which are advantageous when we are studying flooded regions for long durations, the data has accurate geo-coding. MODIS data is well distributed via Earth observation Station (EOS) gateway[12].

The MODIS satellite image of level-2 product is used which is atmospherically, radio-metrically and geometrically corrected. From this satellite image product, we have extracted band-2 of the satellite image using the geo-locations which covers the flooded scene for our study. In classical water detection techniques like (NDVI) Normalized Difference Vegetation Index[9–11] is used distinguish between vegetation, water and bare soil. The problem with NDVI is not proper separation of vegetation pixels with water pixels. NDVI test is not always enough to identify water pixels, as one has to apply more tests or advance methodology to detect clear water and differentiating remote clouds and cloud shadows[9]. Classical detection methods are error prone, time consuming and needs supervision for training dataset. The proposed automatic unsupervised methods are devised in creating water masks on the satellite images and which is much faster, easier and accurate in creating water mask on satellite images. Automatic water extraction techniques are used for multi-temporal satellite images at three different stages like before, during and after flooding.

2. Background Study

Several research works have been carried-out in European countries[9], America[13], Asian countries like India[11] china[2] and Thailand[14] using satellite images on flood assessment. In India, floods[6,7] are common in some regions like- Brahmaputra basin in Assam, Godavari basin and Krishna basin in Andhra Pradesh, Kosi basin in Bihar and Yamuna basin around Delhi etc. The flood factors like location, inundated areas of long periods and durations can be studied by using remote sensed data. Freely available optical satellite images[8] like MODIS (Moderate Resolution Imaging Spectro radiometer) are regularly made used by researchers in flood assessment. MODIS images are widely used in hydrological applications[9] like flood detection, characterization and warning flood disaster response and damage assessment and wide coverage areas.

Rajiv Kumar Nath *et al.*[10] for water body extraction from satellite images several methods like support vector machine, Bayesian and fuzzy Gustafson-Kessel (FGK) are used. J. Senthilnath *et al.*[11] have used supervised methods like artificial neural network and support vector machine for extracting flooded regions from the satellite image. They have used MODIS satellite image to differentiate flooded regions with non-flooded regions. Chenghu Zhou *et al.*[2] have used supervised methods like radial basis function for extracting water image pixels from Radar sat image and AVHRR image. Supervised methods are mostly being used by researchers for flood application but there is an existence of performance limitation due to availability or collected ground truth data. Hence researchers are working towards unsupervised techniques in this context. A clustering method will automatically assigns pixels to respective spectral clusters. The property of clustering algorithm is to group individuals in a population of data such that the outcome is a partitioning of data set .Some of the researcher who have used unsupervised methods in their work are Gheogrhe Stancalie *et al.*[15] has carried out research on different remote sense data for flood disaster assessment and flood risk reduction application. Xiangyun Hu *et al.*[16] have used region based unsupervised techniques for segmenting water bodies from land surface features. Only a few unsupervised methods like ISO-DATA, K-means clustering technique have been carried out in flood assessment application and also the results obtained depend on number of clusters which are initialized and some are semi-automatic.

In this paper, we have used image clustering methods like-mean shift and self organization maps. These methods are used for the identification of water pixels from the multi-temporal satellite images. Multi-temporal analyses are carried out using different dated imaging and results are validated using performance evaluation methods. Our research is on exploring unsupervised methods using MODIS satellite images in extracting water pixels and also distinguishing flood region with non-flood regions from satellite images.

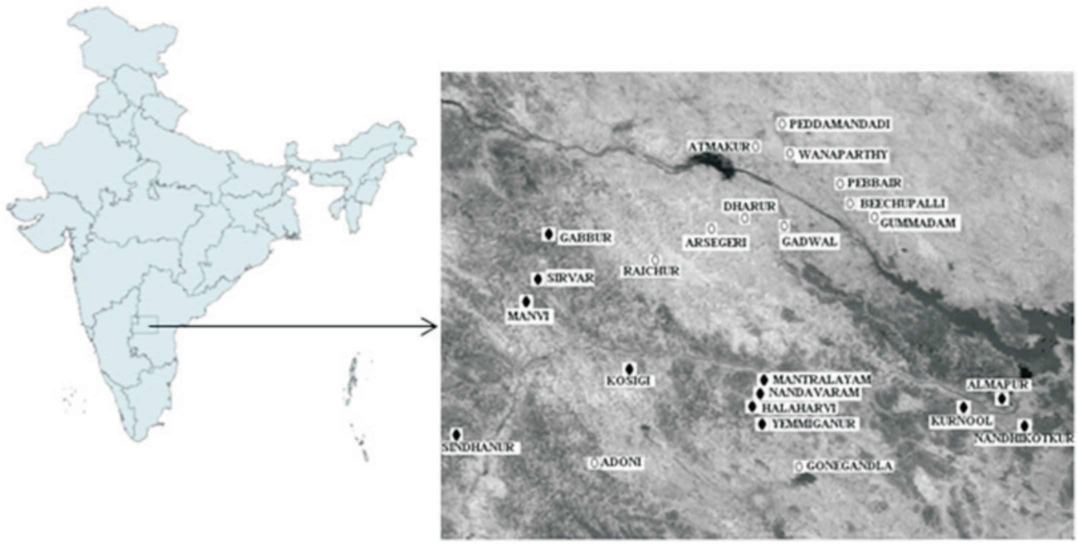

Fig. 1. Shows Flooded (represented with black dot) and Non-flooded Regions (represented with white dot) which are used in Current Study.

Table 1. The Table shows 12 Numbers of Flooded and Non-flooded Places.

Flooded			Non-Flooded		
1) Kosigi	2) Sindhanur	3) Mantralayam	1) Atmakur	2) Peddamandadi	3) Wanaparthy
4) Nandavaram	5) Halaharvi	6) Yemmiganur	4) Pebbair	5) Beechupalli	6) Gummadam
7) Kurnool	8) Alampur	9) Nandhikotkur	7) Gonegandla	8) Adoni	9) Raichur
10) Gabbur	11) Sirvar	12) Manvi	10) Arsegiri	11) Dharur	12) Gadwal

3. Study Area

The study area details are discussed in this section. We have chosen Krishna and Tungabhadra rivers regions. During September-2009 rivers region received heavy rainfall causing floods. In our research we use MODIS (MOD09Q1) Terra Surface Reflectance 8-Day L3 Global 250 $mtrs^2$ satellite images[12]. Three different dated images like before (Mar-2009), during (Sept-2009), after (Nov-2009) are considered from MOD09Q1-MODIS satellite product. MOD09Q1 has two bands namely upper band which is centered between 620–670 nm and lower band which is centered between 841–876 nm. The classifications of water pixels are due to the spectral characteristics of the band 2 data (841–876 nm). The satellite image area coverage is 3, 13,568 sq mtrs. In the Fig. 1, we have shown the study area of flooded and non-flooded places identified on a satellite image. The lists of places which were indented and non- indented with floods are given in Table 1.

For our study, we have chosen MODIS march, Sept and Nov month image which is shown in the Fig. 2. Here we have taken same area coverage of the flooded places.

4. Methodology

A block diagram of automatic water detection using multi-temporal satellite image analysis is shown in the Fig. 3.

4.1 Preprocessing

Pre-processing is essential step for automatic water extraction processing. During pre processing noise removal/ reduction is done. Noise removal helps in enhancing the image quality. The satellite images during flood times are

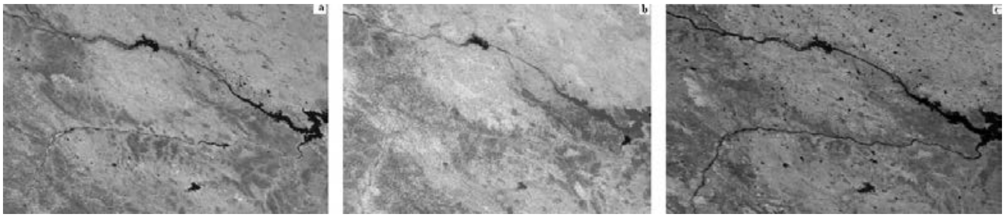

Fig. 2. (a) Original Modis Satellite Image of Krishna River Region before Flood (March 2009); (b) Original Modis Satellite Image of Krishna River Region during Flood (September 2009) and (c) Original Modis Satellite Image of Krishna River Region after Flood (November 2009).

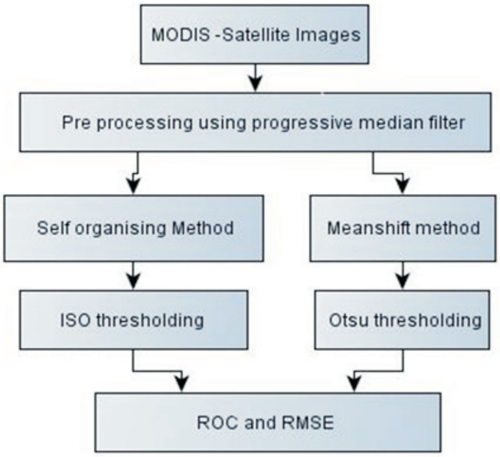

Fig. 3. Block Diagram of Flood Assessment.

susceptible to noise in the form of clouds. To overcome these effects, filtering is done. Progressive median filter[17] are used to remove spectral reflectance of vegetation and water, which are almost equal (which appears similar) and also helps to remove outliers and maintain image sharpness. This helps in preserving elongated edges for the image for segmentation.

4.2 Segmentation technique

The image segmentation techniques[16] are used for extracting the desired features like texture and shape from an object. In this paper, mean shift (MS) and Self organizing Maps are used as segmentation techniques.

4.2.1 Meanshift

MS is a popular unsupervised method which is based on kernel density estimation[18]. Mean shift Segmentation which is applied on satellite image will helps in identifying non-linear river water network feature in the image. Mean Shift picks random point in the feature space and converge towards local maximal density. Based on weighted average, the mean is shifted and iteratively identify the similar density pixels. Local point of convergence is calculated using Gaussian kernel

$$\hat{f}(X) = \frac{1}{nh_i^d} \sum_{i=1}^{n} k \left\| \frac{(X - X_i)}{h_i} \right\|^2 \tag{1}$$

The data points X_i, where $i = 1, 2, 3 \ldots n$ are in d-dimensional space R^d, bandwidth parameter h_i where $h_i > 0$ is used for calculation of kernel density estimation at location x. The kernel k is a Gaussian kernel which satisfies the condition

$$K(x) = c_{k,d} k(\|x\|^2) > 0$$
$$\text{where: } \|x\| \leq 1 \tag{2}$$

The Gaussian kernel $G(x)$ is defined as $G(x) = c_{k,d} k(\|x\|^2)$.

The property of kernel profile has been verified using gradient of an equation;

$$m_G(X) = c \frac{\nabla \hat{f_k}(x)}{\hat{f}(x)} \tag{3}$$

where: $m_G(X)$ is the mean shift vector, 'C' a positive constant and gives the location x. The mean shift vector is defined as:

$$m_{h,G}(x) = \frac{\sum_{i=1}^{n} x_i g\left(\frac{\|x-x_i\|^2}{h}\right)}{\sum_{i=1}^{n} g\left(\frac{\|x-x_i\|^2}{h}\right)} - x \tag{4}$$

Mean shift vector computed with Gaussian kernel G is proportional to the normalized density gradient estimate obtained with the Gaussian kernel.

Mean shift vector will indicate the direction of maximum increase in density. The mean shift is obtained by successive computation of the mean shift vector and translation of Gaussian kernel $G(x)$ by the mean shift vector. Finally, it converges at a nearby point where the estimate has zero gradients and iterative equation is given by:

$$y_{i+1} = \frac{\sum_{i=1}^{n} x_i g\left(\|\frac{x-x_i}{h}\|^2\right)}{\sum_{i=1}^{n} g\left(\|\frac{x-x_i}{h}\|^2\right)}$$
$$j = 1, 2, 3 \ldots n \tag{5}$$

Initial position of the kernel is chosen as one of the data point's x_i. Usually, the local maxima/modes the density is the convergence points of the iterative procedure. The mean shift technique is based on unsupervised clustering.

4.2.2 Self Organizing Maps (SOM)

A SOM is characterized by the input patterns[19–21] for topographic map wherein the spatial location (i.e. coordinates) of the neurons is essential for statistical features present in the input patterns, hence the name "Self organizing map". SOM feature map consists of a 2D array units and each unit is fully connected via 'n' weights to the n-dimensional input pattern. SOM are characterized by the topographic map formation[19] with the input patterns in which the random samples of the image are drawn as training samples for similarity matching and iteratively it is carried out in forming groups and resultant groups are delineated to get the clusters.

Steps of Self organizing Maps are summarized as follows:

Step 1) Initialization: In this, we initially choose 50 random values for given image and term it as initial weight vectors – wj (0). The initial weight vector is wj (0) and it should be different for $j = 1, 2 \ldots 1$ where: l –number of neurons for finding the magnitude of the weights. The initial points are used for training samples for segmenting water pixels.

Step 2) Sampling: A sample x is drawn from the input space with a probability density function. Here vector x represents the activation pattern which is applied to lattice. The dimension of the vector x is equal to m (dimension of the input data space).

Step 3) Similarity matching: The best matching neuron $i(X)$ is found out through the iterations, at each step of 'n' i.e. using function called minimum distance Euclidean

$$i(X) = \text{arg minj } \|X(n) - Wj\| \quad \text{where} \quad j = 1, 2, 3 \ldots 1 \tag{6}$$

Step 4) Updating: The synaptic weight vector is updated using

$$Wj(n+1) = Wj(n) + \acute{\eta}(n)hj, i(X)(n)(X(n) - Wj(n)) \tag{7}$$

where: $\acute{\eta}(n)$ is the learning rate parameter and $hj, i(X)(n)$ is the neighboring function centered around the neuron $i(x)$. Here $\acute{\eta}(n)$ and $hj, i(X)\ (n)$ vary dynamically.
Step 5) Continuation: The sampling is continued until feature map is observed.

4.3 Thresholding

We have used thresholding technique[22,23] for extracting water image pixels from other pixels. After applying mean shift we have used Otsu thresholding method to extract water pixels and similarly for SOM we have used ISO-Data binarization thresholding method to extract water image pixels.

5. Performance Evaluation

In this section, the performances of automatic water extraction techniques on multi-temporal satellite images are measured. The extracted results using mean shift and SOM are compared with the ground truth images in order to verify their precision we have used two indices for evaluating the methods performances for segmentation[24]. They are;

1) Root means square (RMSE)
2) Receiving of characteristics (ROC)

5.1 Root means square error

RMSE[11] is the statistical measure of varying quantity of magnitude

$$\text{RMSE} = \sqrt{\frac{1}{N}\sum_{k=1}^{N} E_k^2} \tag{8}$$

where: E_K- the error between the ground truth data and actual output of the algorithm implemented and 'N' is the pixel count.

5.2 Receiver operating characteristics

Receiver Operating Characteristics[24] has parameters like TPR, TNR, FPR and FNR which is calculated for the pre flood and post flooded satellite images for performance evaluation of the algorithm[11].

a) Sensitivity or True Positive Rate (TPR)

$$\text{TPR} = \frac{TP}{(TP + FN)} \tag{9}$$

b) Specificity or True Negative Rate (TNR)

$$\text{TNR} = \frac{TN}{(TN + FP)} \tag{10}$$

c) False Positive Rate (FPR)

$$\mathrm{FPR} = \frac{FP}{(FP + TN)} \tag{11}$$

d) Accuracy (ACC)

$$\mathrm{ACC} = \frac{(TP + TN)}{(TP + FP + TN + FN)} \tag{12}$$

In the flooded satellite image, the ROC parameter is applied to locate the flooded places. A place which are positive according to the ground truth data and also according algorithm computed result is a True Positive (TP). The place which is positive according to the algorithm computed results but negative according to the ground truth data is a False Positive (FP). Likewise, a place which is negative according to the ground truth data and also according to algorithm computed result is a True Negative (TN).While the place which is negative according to the algorithm computed result but positive according to the ground truth data is a False Negative (FN). For both pre and post flooded images ROC parameters are applied in order to calculate the accuracy of the extraction by algorithms. ROC parameters are useful in order to determine the algorithmic performance & comparison of algorithms.

6. Results and Discussions

In result and discussion section, the results obtained and comparative analysis is discussed. In this paper, multi-temporal time series for the MODIS data for the Krishna and Tungabhadra rivers, south India are carried-out using mean shift and SOM image processing algorithms and compared with each other to evaluate their performance. The experiments were conducted on Intel i5 windows 7 system using Matlab 7.12.

From the Fig. 4, we have shown 12 flooded and non-flooded places. The ground truth information is taken with respect to survey data[25]. We can observer that cities which are near and far to river banks have flooded. So challenge in identifying flooded places using image processing plays important role. For this reason we have used unsupervised methods in locating non-flooded places.

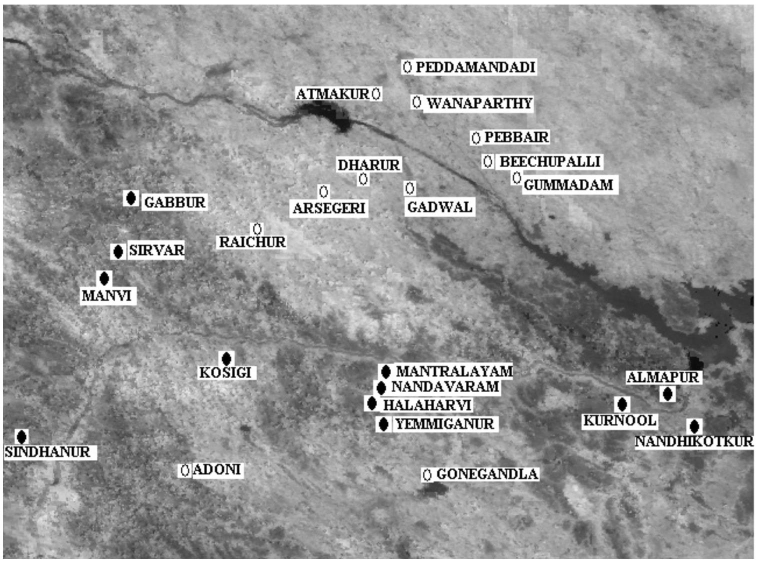

Fig. 4. Ground Truth Information of the Terrain Around River Krishna in the Month of September 2009. Towns which are Flooded are Shown using Black Dots and Cities which are Non-flooded are Shown using White Dots.

The ground truth information is prepared for March and November 2009 image because to compare with extracted results and evaluate using RMSE parameter. From the Fig. 5 we see that river lane is extracted and compared with Fig. 6(a) and 6(c).

We have applied ROC parameter for calculating mean shift and SOM extraction performance results. Tables 2 and 3 shows the values. For the March month, SOM extraction results are 98% with respect to ground truth data while mean shift results are 97%.

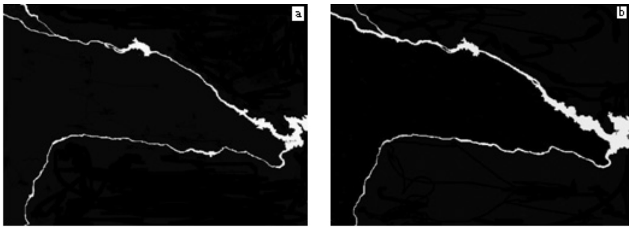

Fig. 5. Ground Truth Information of the Terrain Around River Krishna River for the Month of (a) March 2009; (b) November 2009.

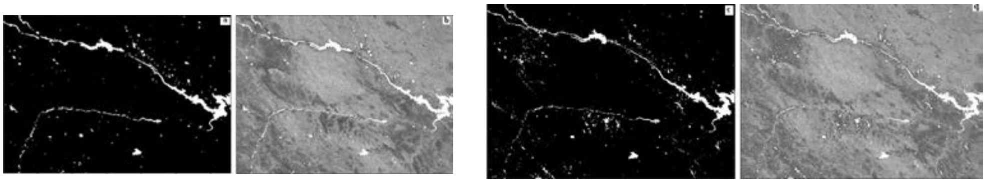

Fig. 6. (a) Segmented March Month Images of Krishna River using Mean Shift; (b) Extracted and Overlaid on the Original Image using Mean Shift; (c) March Month Images of Krishna River using SOM and (d) Extracted and Overlaid on the Original Image using SOM.

Table 2. Shows the ROC Parameter Value of Calculating Accuracy of Extraction using Mean Shift and SOM Algorithm for the March Month.

Algorithm	TN	FN	FP	TP	Sensitivity/ TPR	Specify/ TNR	FPR	Accuracy
Mean shift	300581	1904	5020	7019	0.7866	0.9835	0.0164	0.9777
SOM	303178	3064	2423	5859	0.6566	0.9920	0.0079	0.9825

Table 3. Shows ROC Parameter Value of Calculating Accuracy of Extraction using Mean Shift and SOM Algorithm for the November Month.

Algorithm	TN	FN	FP	TP	Sensitivity/ TPR	Specify/ TNR	FPR	Accuracy
SOM	297940	3670	3706	8252	0.6921	0.9877	0.0122	0.9765
Mean shift	294634	1718	7012	10204	0.8558	0.9767	0.0232	0.9721

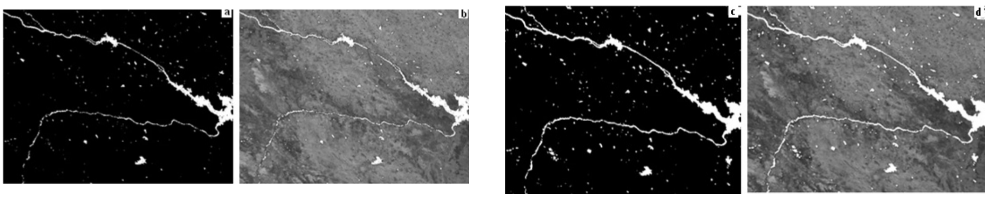

Fig. 7. (a) Segmented November Month Images of Krishna River using Mean Shift; (b) Extracted and Overlaid on the Original Image using Mean Shift; (c) November Month Images of Krishna River using SOM and (d) Extracted and Overlaid on the Original Image using SOM.

Table 4. Shows the RMSE Value between Extracted and Ground Truth Data.

RMSE	March month	November Month
Self Organizing Maps	0.1200	0.1348
Mean shift	0.1376	0.1510

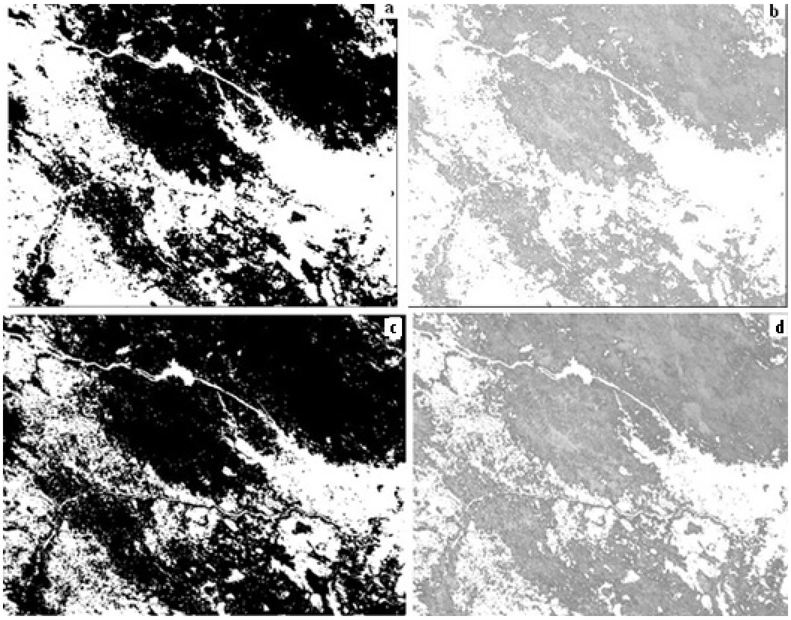

Fig. 8. Original Image of River Krishna during Flood (September 2009), (a) Segmented September Month Images of Krishna River using Mean Shift; (b) Extracted and Overlaid on the Original Image using Mean Shift; (c) September Month Images of Krishna River using SOM and (d) Extracted and Overlaid on the Original Image using SOM.

For the November month image results of SOM is nearly 97.65 % while mean shift result is about 97.21%. So from Tables 2 and 3, we see that results of SOM are better than mean shift.

The RMSE values in the Table 4 are computed keeping ground truth data with extracted results as shown in the Figs. 4, 5 (a and c) and 6 (a and c). From the Table 4 it is clear that SOM has works better than mean shift. The RMSE value of SOM is very less in comparison with mean shift algorithm, so this proves SOM is better algorithm than Mean shift.

During flooded image extraction results obtained by using mean shift and SOM are shown in the Fig. 8. From the Fig. 8, we can see that water has spread out near to river banks and also other regions. So this becomes important challenge in determining water image pixels by image processing techniques.

Mean shift is used for both filtering and segmentation. The filtering can be explained with each pixel represented as vector that combines both image locations pixels values and assigns each pixel with value of the nearest maximal density location to merge vectors. By using gradient ascent method, maximum density points clustered for identifying local maximum of a kernel-density. With kernel function-k convergence is achieved then Otsu thresholding is applied. The results of mean shift extraction are shown in the Fig. 8(a) and 8(b). In SOM, initially some random points are chosen. These initial points are used for similarity matching from the original image. The local characteristic of the original image like pixel value are taken into account, then iteratively the similar pixel values move towards mean and a converged mean is obtained. The segmented/converged image is used with ISO thresholding method for extraction. The results of SOM extraction are shown in the Fig. 8(c) and 8(d).

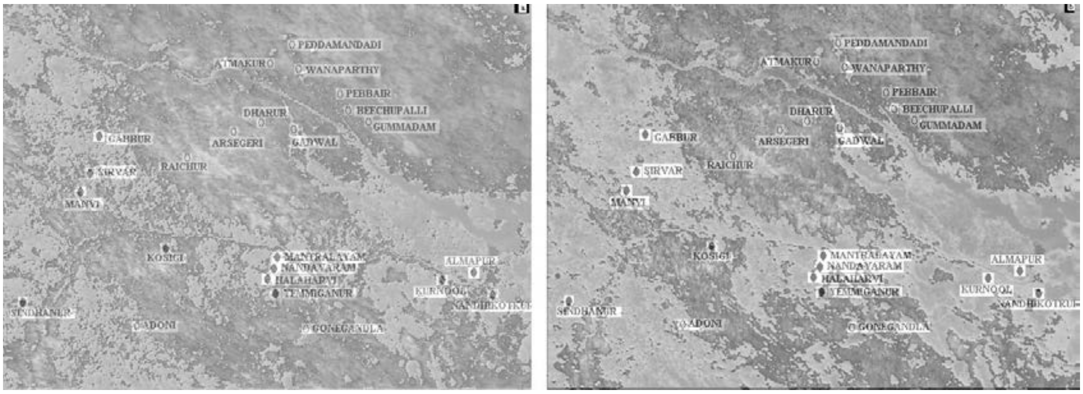

Fig. 9. (a) Showing SOM Results Overlaid with the Original Image; (b) Showing Mean Shift Results Overlaid with the Original Image.

6.1 Comparative analysis of segmentation algorithms

The detailed comparison of algorithms is shown using before, during and after satellite images for the given flooded scene.

6.1.1 March satellite image analysis

Mean shift and SOM algorithms are applied for before flooded march image and applied results are shown in the Fig. 5. Here we can see the river lane is extracted using both algorithms and verified with the ground truth data. Here water image pixels are extracted from satellite image using mean shift by setting parameter hr and hs to value 10. Then we have used Otsu method for thresholding the image. In case of Self Organizing Method, initially 50 random values used from the image are drawn as sample as a part of initialization. And thresholding of 0.05 values is set for grey level of the image iteratively to separate image in order to two discriminate land and water classes as shown in Fig. 5(c) and 5(d). Further segmented results are compared with ground truth data using RMSE value.

6.1.2 September month satellite image analysis

Mean shift and SOM methods are applied for during flood September month, which is shown in the Fig. 9. Here we have extracted water image pixels to verify flooded and non-flooded places. After extraction, ROC parameter is used to determine the accuracy. We found that SOM has identified flooded places better in comparison with Mean shift. Figure 9 (a) and 9(b) shows the extracted and overlaid results by SOM and MS in order to determine flooded places.

In during flooded image, the water pixels are distributed over the entire region so in grouping them the threshold value should be set to higher values. In case of during flooded image, we have identified total 24 places in which 12 places are flooded regions and 12 places are non flood regions, as in the Fig. 3. Here we cannot prepare the ground truth data because water pixels are scattered in the image and it becomes hard to intervene from grouping water pixels. The ROC parameter for during flooded image is calculated as shown in the Table 5, SOM has performed well in marking both flooded and non-flooded regions with compared to mean shift.

Here we have overlaid the extracted image with original map in order to verify identified places. From the Table 5, we can see that SOM has performed better than Mean shift algorithm.

6.1.3 November month satellite image analysis

Mean shift and SOM algorithms are applied for before flooded march image and applied results are shown in the Fig. 5. Here we can see the river lane is extracted using both algorithms and verified with the ground truth data. Here water image pixels are extracted from satellite image using mean shift by setting parameter hr and hs to value 10.

Table 5. Shows ROC Parameter Applied for During Flooded Image. (a) ROC Parameter Applied for During Flooded Image using SOM Method, (b) ROC Parameter Applied for During Flooded Image using Mean Shift Method.

SOM	ROC Parameters	
	TP	12
	TN	11
	FP	1
	FN	0

Mean Shift	ROC Parameters	
	TP	10
	TN	9
	FP	3
	FN	2

Then we have used Otsu method for thresholding the image. In case of Self Organizing Method, initially 50 random values used from the image are drawn as sample as a part of initialization. And thresholding of 0.05 values is set for grey level of the image iteratively to separate image in order to two discriminate land and water classes as shown in Fig. 5(c) and 5(d). Further segmented results are compared with ground truth data using RMSE value.

7. Conclusions

In this paper, we are analyzing flood assessment using MODIS satellite image by unsupervised techniques like mean shift and SOM for water image pixel identification and extraction. The SOM algorithm has performed well for in all these cases before, during and after flood images. We determine algorithm performance based on the parameters like ROC. These parameters are applied for algorithm results and validated it against the ground truth image. In case of during flood image, the ROC performance evaluation parameter is used for identifying non-flooded regions and flooded regions to record the flood database. Finally we conclude that a SOM method has performed better in extraction of flooded regions compared to conventional unsupervised method like mean shift.

Acknowledgements

This research work is supported by Space Technology Cell, Indian Institute of Science (IISC) and Indian Space Research Organization (ISRO) grant.

References

[1] J. A. Walkey, Development of a Change Detection Tool for Image Analysis, *MS thesis. University of Wisconsin-Madison*, (1997).
[2] Chenghu Zhou, Jlancheng Luo, CunJlan Yang, Baolln Ll and Shlxln Wang, Flood Monitoring using Multi-Temporal AVHRR and RADARSAT Imagery, *Photogrammetric Engineering & Remote Sensing*, pp. 633–638, May (2000).
[3] X. Zhang, R. Sun, B. Zhang and Q. Tong, Land Cover Classification of the North China Plain using MODIS EVI Time Series, *ISPRS Journal of Photogrammetry and Remote Sensing*, vol. 63, pp. 476–484, (2008).
[4] W. J. W. Van and R. R. Root, Hyper Spectral Analysis of Multi-Temporal Landsat TM Data for Mapping Fuels in Yosemite National Park, *Proceedings of Joint Fire Science Conference and Workshop, Boise*, Idaho, June (1999).
[5] N. Verhoest, P. A. Troch and T. F. P. De, Spatial Soil Moisture Mapping through Multi-Temporal Analysis of ERS-SAR PRI Data, *3rd ERS SYMPOSIUM*, Florence, (1997).
[6] P. R. Rakhecha, Highest Floods in India, The Extremes of the Extremes: Extraordinary Floods edited by Árni Snorrason, Helga P. Finnsdóttir, Marshall E. Moss, *IAHS publication*, no. 271, ISSN 0144-7815, p. 167.
[7] O. N. Dhar and Shobha Nandargi, Hydro Meteorological Aspects of Floods in India, *Natural Hazards*, vol. 28, pp. 1–33, Kluwer Academic Publishers, (2003).
[8] Ashbindu Singha, Digital Change Detection Techniques using Remotely-Sensed Data, *International Journal of Remote Sensing*, vol. 10(6), pp. 989–1003, (1989).
[9] R. Brakenridge and E. Anderson, Modis-Based Flood Detection, Mapping and Measurement: The Potential for Operational Hydrological Applications, *NATO Science Series*, 1, vol. 72, *Transboundary Floods: Reducing Risks through Flood Management*, vol. 1, pp. 1–12.
[10] Rajiv Kumar Nath and S. K. Deb, Water-Body Area Extraction from High Resolution Satellite Images-An Introduction, Review, and Comparison, *International Journal of Image Processing (IJIP)*, vol. 3(6), pp. 265–384, January (2010).
[11] J. Senthilnath, Shivesh Bajpai, S. N. Omkar, P. G. Diwakar and V. Mani, An Approach to Multi-Temporal MODIS Image Analysis using Image Classification and Segmentation, *Advances in Space Research*, (2012).
[12] E. F. Vermote, S. Y. Kotchenova and J. P. Ray, MODIS Surface Reflectance User's Guide, MODIS Land Surface Reflectance Science Computing Facility, Version 1.2 June (2008).

[13] Bruce L. Rhoads, Flood Hazard Assessment for Land-Use Planning Near Desert Mountains, *Environmental Management*, vol. 10(1), pp. 97–106, Springer.
[14] Pengyu Chen, Flood Impact Assessment using Hydrodynamic Modelling in Bangkok, Thailand, Technical Report, March (2007).
[15] Gheorghe Stancalie, Simona Catana, Anisoara Irimescu, Elena Savin, Andrei, Diamandi, Alina Hofnar and Simona Oancea, Contribution of Earth Observation Data Supplied by the New Satellite Sensors to Flood Management, *Transboundary Floods: Reducing Risks through Flood Management*, p. 287.
[16] Xiangyun Hu, C. Vincent Tao and Björn Prenzel, Automatic Segmentation of High-resolution Satellite Imagery by Integrating Texture, *Intensity, and Color Features, Photogrammetric Engineering & Remote Sensing*, vol. 71(12), pp. 1399–1406, December (2005).
[17] Zhou Wang and David Zhang, Progressive Switching Median Filter for the Removal of Impulse Noise from Highly Corrupted Images, *IEEE Transactions on Circuits and Systems—II: Analog and Digital Signal Processing*, vol. 46(1), January (1999).
[18] Dorin Comaniciu and Peter Meer, Mean Shift Analysis and Applications, *The Proceedings of the Seventh IEEE International Conference on Computer Vision*, (1999).
[19] Teuvo Kohonen, The Self-Organizing Map, *Neurocomputing*, vol. 21(1–3), pp. 1–6, 6 November (1998).
[20] M. G. Prasad, S. N. Omkar and V. Mani, Comparative Study of Neural Network Approach and Genetic Programming Approach to Land Cover Mapping, *Fifth International Conference – World Scientific and Engineering Academu and Society*, Udine, Italy (2004).
[21] Jander Moreira and Luciano Da Fontoura Costa, Neural-Based Color Image Segmentation and Classification using Self-Organizing Maps, *Anais do IX SIBGRAPI*, pp. 47–54, (1996).
[22] Abderrahmane Kefali, Toufik Sari and Mokhtar Sellami, Evaluation of Several Binarization Techniques for Old Arabic Documents Images.
[23] Joan S. Weszka, Survey: A Survey of Threshold Selection Techniques, *Computer Graphics and Image Processing*, vol. 7(2), pp. 259–265, (1978).
[24] Tom Fawcett, An Introduction to ROC Analysis, *Pattern Recognition Letters*, vol. 27, pp. 861–874, (2006).
[25] Tom Fawcett, ROC Graphs: Notes and Practical Considerations for Researchers, HP Laboratories.